Appl. Phys. B 71, 197–201 (2000) / Digital Object Identifier (DOI) 10.1007/s003400000339

Applied Physics B
Lasers
and Optics

Transient conical parametric scattering of two orthogonally polarized waves in $BaTiO_3$

P. Jullien[1], **F. Bezançon**[1], **P. Mathey**[1], **S. Odoulov**[2]

[1] Laboratoire de Physique, Matériaux pour l'Optique non linéaire, UMR CNRS 5027, Université de Bourgogne, BP 47870, 21078 Dijon, France
(Fax: +33-80/39-5961, E-mail: pjullien@u-bourgogne.fr)
[2] Institute of Physics, National Academy of Sciences, 03 650 Kiev-22, Ukraine
(Fax: +380-44/265-2359, E-mail: odoulov@iop.kiev.ua)

Received: 27 March 2000/Published online: 16 June 2000 –

Abstract. The strength of the transient parametric scattering in $BaTiO_3$ is shown to be strongly dependent on the initial conditions of the sample illumination. It is shown that the effect can be explained by a considerable increase of the seeding radiation intensity after pre-exposure of the sample to the ordinarily polarized pump beam.

PACS: 42.65.-k; 42.65.Hw; 42.65.Yj

Two coherent light waves, one ordinary and the other extraordinary, propagating in a plane normal to the optical axis of a barium titanate crystal give rise to conical light-induced scattering described in [1–4]. It has been shown that the light emission along the conical surface is a consequence of the parametric mixing of four waves: two pump waves (with the wavevectors $\boldsymbol{k}_{\mathrm{p}}^{\mathrm{o}}$ and $\boldsymbol{k}_{\mathrm{p}}^{\mathrm{e}}$) and two scattered waves (with the wavevectors $\boldsymbol{k}_1^{\mathrm{o}}$ and $\boldsymbol{k}_2^{\mathrm{o}}$) meeting the following phase matching condition:

$$\boldsymbol{k}_{\mathrm{p}}^{\mathrm{o}} + \boldsymbol{k}_{\mathrm{p}}^{\mathrm{e}} = \boldsymbol{k}_1^{\mathrm{o}} + \boldsymbol{k}_2^{\mathrm{o}} \,. \tag{1}$$

Here the subscripts label the pump waves (p) and scattered waves (1, 2), respectively, while the superscripts o, e define the light polarization (ordinary and extraordinary waves, respectively).

Equation (1) imposes the angular distribution for scattered light to be restricted by the conical surface with the apex angle which depends on the pump angle and on the crystal birefringence [1, 2]. Both, the experiment and the calculations show a rather unusual feature: the temporal dynamics of the scattered light strongly depends on the direction of the scattering. The scattering cone can be divided into four parts by two planes, one defined by the wavevector of the first pump wave $\boldsymbol{k}_{\mathrm{p}}^{\mathrm{o}}$ and crystal *C*-axis and the other defined by the wavevector of the second pump $\boldsymbol{k}_{\mathrm{p}}^{\mathrm{e}}$ and crystal *C*-axis. Those parts of the scattering cone that are within the angular window limited by these two planes exhibit the bright steady-state scattering. The light scattered out of the mentioned angular window is visible only during a relatively short time after the beginning of the exposure and it vanishes in the steady state.

Figure 1a shows the steady-state far-field distribution of the scattered light on the screen placed behind the $BaTiO_3$ sample. The vertical lines drawn through the dots marking the position of the pump waves in Fig. 1b separate the parts of the scattering ring with the steady-state scattering (between two

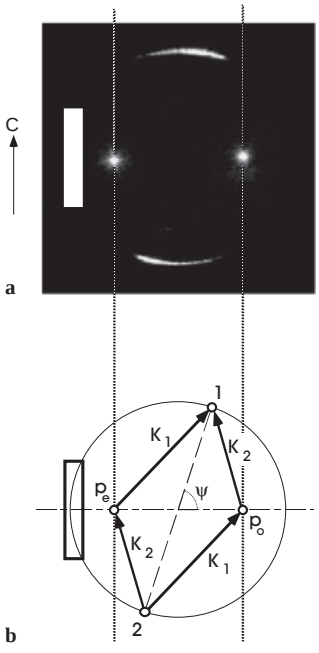

Fig. 1a,b. The steady-state scattering pattern for $BaTiO_3$ sample exposed to two orthogonally polarized light beams (**a**) and grating vector diagram for this process (**b**). The *dots* $\boldsymbol{p}_{\mathrm{o}}$ and $\boldsymbol{p}_{\mathrm{e}}$ show the tips of the wavevectors of the ordinary and extraordinary pump waves, respectively, while the *dots* 1 and 2 mark the position of an arbitrary pair of the conjugate scattered waves on the scattering ring. The *dotted lines* separate the directions with the nonvanishing steady-state scattering (between the two *lines*) from the directions with only transient scattering (all other directions). The *vertical slit* shows the angular window from where the scattered light is collected to the detector in our experiment

lines) from the parts with only transient scattering (outside two lines).

The grating vector diagram for the considered process is shown in Fig. 1b. The dots 1 and 2 show a pair of conjugated components on the cone of scattered light while $\boldsymbol{K}_1$ and $\boldsymbol{K}_2$ show the grating vectors of the gratings recorded by the ordinary pump wave $\boldsymbol{p}_o$ and the scattered waves 1 and 2. The ring shows all possible directions of propagation of the scattered light.

The theory developed in [2, 3] gave a complete description for the steady state and transient behaviour. The experimental results fit qualitatively well with the calculated ones. Reasonable semiquantitative agreement was demonstrated in [3] with only one fitting parameter (the effective electrooptic constant) for the available $BaTiO_3$ sample.

In the present paper we describe a new unexpected feature for this type of parametric mixing: It has been found that the dynamics of the transient scattering strongly depends on the initial conditions, i.e., it is different for a virgin sample (where all photorefractive gratings are totally erased by an incoherent light beam) and for a sample pre-exposed to one of the two pump waves. This difference is attributed to different starting levels of the radiation seeding the non-linear scattering.

1 Experiment

A sample of $BaTiO_3$ measuring $3.6 \times 6.1 \times 6.0\,\mathrm{mm}^3$ is placed in such a way that its ferroelectric axis points up, being normal to the optical table surface. The measured absorption constants for this sample are $\alpha_0 = 1.99 \pm 0.05\,\mathrm{cm}^{-1}$ and $\alpha_e = 2.32 \pm 0.05\,\mathrm{cm}^{-1}$ at $\lambda = 514\,\mathrm{nm}$. The 514-nm radiation of the single-mode single-frequency Ar^+ laser is used to form the two pump waves (Fig. 2). The phase retarder ($\lambda/2$) placed in one of the two beams rotates the linear polarization roughly to 90°. The precise adjustment of polarization of the incident waves (one extraordinary and other ordinary wave of the crystal) is made with two polarizers P. With the polarizer placed in front of the sample the phase retarder ($\lambda/2$) can be used to control the input intensity of this pump. The intensity of the ordinarily polarized pump wave is controlled using a phase retarder and a polarizer.

The detector D1 measures the intensity of the pump wave while D2 monitors the intensity of the scattered light. A PC-based data acquisition system is used to collect and process the data.

At first we compare the dynamics of the transient light-induced scattering for different initial conditions adjusting the detector D2 to measure the brightest part of the transient scattering. Special care is taken to minimize the stray light collected by the detector. For this purpose, a polarizer sheet placed in front of the detector (not shown in the figure) selects the ordinarily polarized light. In addition, spatial filtering is used to collect the light propagating mainly in the phase-matched direction (see the position and dimensions of the vertical slit in Fig. 1a,b).

The intensities of the ordinary and extraordinary pump waves are $5.7\,\mathrm{W/cm}^2$ and $6.3\,\mathrm{W/cm}^2$, respectively, with the full pump crossing angle in air $\approx 60°$. The transient peak intensity is about 10^{-5} of the total pump intensity in saturation.

Three different natural initial conditions are possible. The virgin sample can be exposed to the two pump waves simultaneously (A), it can be pre-exposed to the extraordinarily polarized pump wave before we switch on the ordinarily polarized pump (B) and vice versa, it can be pre-exposed to the ordinarily polarized beam (C).

In Fig. 3 the temporal dependence of the light intensity is shown, measured for these three cases with the detector D2.

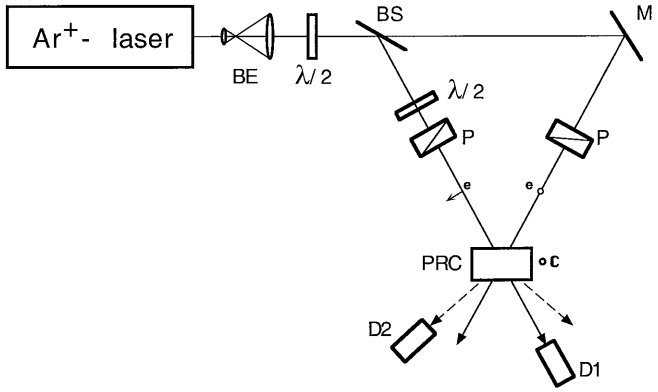

Fig. 2. Schematic representation of the experimental set-up. BE is the beam expander, BS is the beam splitter, M is a mirror, P are the polarizers, $\lambda/2$ are the phase retarders, PRC is the photorefractive crystal, and D1, D2 are the detectors

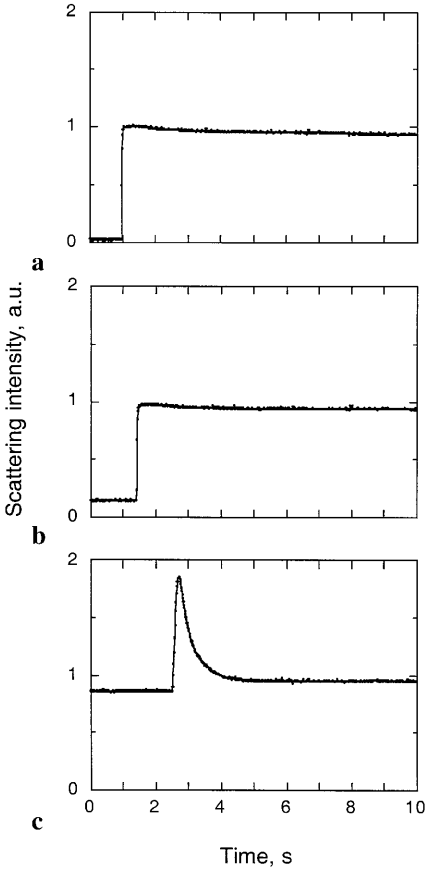

Fig. 3a–c. Time evolution of the scattered light intensity measured in the angular window shown by the vertical slit in Fig. 1. Both pump waves are switched on simultaneously (**a**). The sample is pre-exposed to the extraordinary pump beam during 60 s before the ordinary pump wave is switched on (**b**). The sample is pre-exposed to the ordinary pump beam during 60 s before the extraordinary pump wave is switched on (**c**)

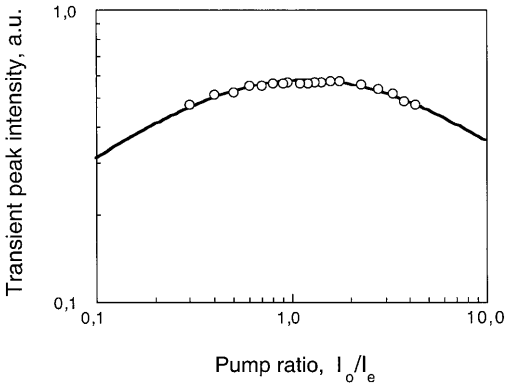

Fig. 4. Log plot of the pump ratio dependence of the transient peak intensity. The *solid line* shows the best fit to (3)

A striking difference in the amplitude of transient scattering is obvious: the strongest effect is observed for the case of pre-exposure to the ordinarily polarized wave (C) whereas nearly nothing is detected with the sample pre-exposed to the extraordinarily polarized light. Note that the saturation value of intensity in all three graphs of Fig. 3 is a background linear scattering which should be taken as a zero value.

It is important to mention that the described enhancement of the transient scattering is observed when the crystal is pre-exposed to the wave identical to that which is used later with the second pump to excite the non-linear scattering. If the pre-exposure is done with the ordinarily polarized wave incident upon the sample at an arbitrary angle no enhancement is observed for the particular direction of interest but transient scattering can appear at other angles.

The amplitude of the transient peak is measured further on for the case (C) as a function of the pump intensity ratio, I_p^o/I_p^e, keeping the intensity of the extraordinarily polarized wave I_p^e constant (Fig. 4). The pre-exposure time is chosen to be 60 s, i.e., it is larger than the dielectric relaxation time even for the smallest intensity of the ordinary pump beam.

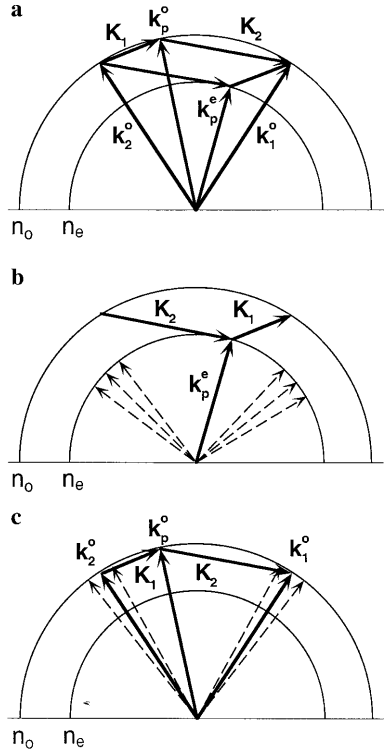

Fig. 5a–c. Wavevector diagrams for **a** parametric scattering with two pump waves, **b** pre-exposure to the extraordinary pump and **c** pre-exposure to the ordinary pump. $\boldsymbol{K}_1$ and $\boldsymbol{K}_2$ are the grating vectors of two gratings which are simultaneously Bragg-matched to the ordinary and to extraordinary pump waves. The *dashed arrows* in B, C are the wavevectors of arbitrary scattered components. Note that the ordinary pump wave can record a grating with grating vector $\boldsymbol{K}_1$ (and $\boldsymbol{K}_2$) together with one of the scattered light components whereas this is impossible for extraordinary pump wave

2 Discussion

Figure 5 shows the phase-matching diagram for the considered scattering process (a) and the wavevector diagrams for the isotropic scattering (no change of polarization of the scattered wave as compared to the incident) of the extraordinary (b) and ordinary (c) waves.

Suppose the seeding wave with the wavevector $\boldsymbol{k}_1^o$ and two pump waves with the wavevectors $\boldsymbol{k}_p^o$ and $\boldsymbol{k}_p^e$ impinge upon the sample. The development of the non-linear scattering starts from the recording of the grating with grating vector $\boldsymbol{K}_2 = \boldsymbol{k}_1^o - \boldsymbol{k}_p^o$ via usual diffusion-mediated charge transport. Diffraction of the ordinary pump wave from this grating is not possible because of the vanishing electrooptic coefficient r_{111}. Quite opposite, the extraordinary wave is efficiently diffracted from the same grating, giving rise to the symmetrically scattered component with the wavevector $\boldsymbol{k}_2^o$. Here the largest $BaTiO_3$ electrooptic coefficient r_{131} is involved in the diffraction, and the polarization of the diffracted wave is orthogonal to that of the extraordinary pump wave (anisotropic diffraction).

In such a manner the photons are injected to the scattered wave 2 and now this wave can record a grating (grating vector $\boldsymbol{K}_1$) together with the ordinary pump wave, one more time via usual diffusion-mediated charge transport.

The appearance of the grating with grating vector $\boldsymbol{K}_1$ gives rise, in turn, to anisotropic diffraction of the extraordinary pump into the initial seeding wave 1 thus increasing its intensity. The non-linear growth of intensities of both scattered waves occurs because of the described feedback. An infinite number of arbitrary pairs of scattered waves like 1 and 2 form the scattering ring as shown in Fig. 1b.

The theory for parametric scattering [3, 4] predicts that any signal wave with the intensity $\boldsymbol{I}_1^o(0)$ meeting the phase-matching condition (1) and propagating in a plane normal to the crystal c-axis will be amplified as:

$$\boldsymbol{I}_1^o(x,\tau) = \boldsymbol{I}_1^o(0,0) \int_0^{2\sqrt{|\Gamma|x\tau}} \exp(-\Delta n^2/4x|\Gamma|n^2)\,[\mathrm{d}\,\mathrm{ber}(\zeta)/\mathrm{d}\zeta]\,\mathrm{d}\zeta\ , \tag{2}$$

with the imaginary coupling constant Γ:

$$\Gamma = \left(2i\,\pi^2 n^4 r_{131} k_B T/\lambda^2 e\right) \times \left(\sqrt{\Delta n/n}\right)\left[\sqrt{\left(I_p^o\, I_p^e\right)}\right]\left[(\alpha_e/\alpha_o)\, I_p^e + I_p^o\right]^{-1}\ , \tag{3}$$

where x is the propagation coordinate, τ the dimensionless time (normalized to dielectric relaxation time), n the refractive index, Δn the crystal birefringence, r_{131} the electrooptic constant, k_B the Boltzmann constant, T the absolute temperature, e the electron charge, θ the pump half-angle inside the sample and ber(ζ) is the zeroth-order Kelvin function (see, for example, [5]). Equation (2) predicts a sharp increase of the scattering intensity in time scale $\tau \approx (1...10)$ and a decay to zero for $\tau \gg 1$(with oscillations for large Γ values). Equation (2) is simplified as compared to that in [2, 3] in the sense that only one of the two possible seeds is considered (one for the signal wave 1 and the other for idler wave 2).

One can see that the intensity of the scattered light is proportional to the intensity of the initial seed $\boldsymbol{I}_1^o(0, 0)$ multiplied to a function describing the temporal behaviour. This last one is also depending on the gain factor Γ given by (3).

Usually, $\boldsymbol{I}_1^o(0, 0)$ is taken to be a small fraction of the input intensity of the ordinarily polarized pump wave:

$$\boldsymbol{I}_1^o(0, 0) = \zeta I_p^o(0) \, . \tag{4}$$

The ζ value accounts for the scattering of the ordinary pump wave from surface and bulk imperfections of the sample and therefore may change from one sample to the other; however it is constant for any particular sample and is independent of the pump beam intensity.

We consider now the meaning of the seeding term $\boldsymbol{I}_1^o(0, 0)$ for the three different initial conditions mentioned above (see also Fig. 3a–c). In case A, when the two pump waves are switched on simultaneously, the seeding radiation is given by (6). The same equation describes, in our opinion, the seed in case B (pre-exposure to the extraordinary pump), what will be discussed later. For the case C (pre-exposure to the ordinary pump wave) the seeding radiation becomes much larger because a set of noisy photorefractive gratings, Bragg-matched to both pump waves, is pre-recorded before the sample is illuminated by the two pump waves.

When the crystal is pre-exposed to the ordinary pump wave the space-charge grating with the grating vector $\boldsymbol{K}_2$ is recorded as well as many other noisy gratings recorded by this pump with scattered components (some of them are shown as dashed arrows in Fig. 5c). The amplitude of the space-charge field E_{SC} for the particular grating with grating vector $\boldsymbol{K}_2$ will be:

$$E_{SC} = mE_D \left[1 - \exp\left(-\Delta\tau\right)\right] \, , \tag{5}$$

where $E_D = \boldsymbol{K}_2(k_B T/e)$ is the diffusion field, $\boldsymbol{K}_2$ the spatial frequency of the grating 2, $\Delta\tau$ is the pre-exposure time normalized to the dielectric relaxation time and m is the contrast of the initial fringe pattern:

$$m = 2\left[\sqrt{\left(\boldsymbol{I}_p^o \boldsymbol{I}_1^o\right)}\right] / \left(\boldsymbol{I}_p^o + \boldsymbol{I}_1^o\right) \approx 2\sqrt{\left(\boldsymbol{I}_1^o / \boldsymbol{I}_p^o\right)} \quad \text{for} \quad \boldsymbol{I}_p^o \gg \boldsymbol{I}_1^o \, . \tag{6}$$

The simple exponential growth of E_{SC} to its saturated value (5) is justified here because the two ordinary waves that are writing each noisy grating are not self-diffracted from this grating ($r_{111} = 0$) and therefore do not change their amplitudes and phases in time.

This space-charge grating results in a grating of high-frequency dielectric constant $\Delta\varepsilon_{13}$ which can be efficiently read-out by the extraordinary pump wave. The diffraction efficiency η of this grating is:

$$\eta \approx (\pi \Delta\varepsilon_{13} \ell / 2n\lambda)^2 \approx \left(\pi n^3 r_{131} \ell m E_D / 2\lambda\right)^2 \left[1 - \exp\left(-\Delta\tau\right)\right]^2 \, . \tag{7}$$

When this grating is read-out by the extraordinary wave with the intensity I_p^e the diffracted wave (ordinary one) has the intensity:

$$\boldsymbol{I}_d^o = \eta \boldsymbol{I}_p^e \approx \boldsymbol{I}_1^o \left(\boldsymbol{I}_p^e / \boldsymbol{I}_p^o\right) \left(\pi n^3 r_{131} \ell E_D / \lambda\right)^2 \left[1 - \exp\left(-\Delta\tau\right)\right]^2 \, . \tag{8}$$

Equation (8) gives the seeding beam intensity that should substitute the factor before the integral in (2) for the sample pre-exposed to the ordinary wave. It differs from the seed defined by (4) by three factors in parenthesis. The first one is a pump ratio which is usually close to one to optimize the intensity of the non-linear scattering in samples with small dichroism. It is mainly the second factor that is responsible for the difference between the seeds in (4) and (8), for the saturated efficiency of the noisy gratings. Taking the handbook values for $r_{131} = 1600 \times 10^{-10}$ cm/V, $n^3 \approx 15$ [6], and $E_D \approx 10^3$ V/cm we can evaluate $\left(\pi n^3 r_{131} \ell E_D / \lambda\right)^2 \approx 10^3$.

This rough estimate shows that the intensity of the seed radiation becomes several orders of magnitude larger when the crystal is pre-exposed to the ordinary pump wave used later to excite the scattering. The difference in the seed intensity results in the difference of the transient scattering for the cases A and C in Fig. 3.

The development of the noisy gratings is not instantaneous in time, so the seeding beam intensity can be controlled by changing the pre-exposure time (8). To check this dependence the transient peak intensity is measured as a function of the pre-exposure time (Fig. 6). The same experimental conditions are kept as described earlier for Fig. 3. The solid line in Fig. 6 shows the best fit of the measured data to (2) and (8). A satisfactory agreement with the described model can be stated. The reasonable value for the dielectric relaxation time $t \approx 3$ s is extracted from this fit. This justifies the choice of pre-exposure time $\Delta\tau = 60$ s for measurements presented in Fig. 4.

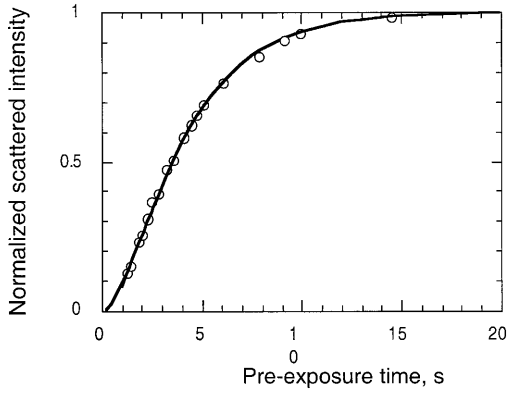

Fig. 6. The measured dependence of transient peak intensity versus pre-exposure time (*dots*) and the best fit to the calculated dependence (*solid line*)

Let us now return to the third possible initial condition when the sample is pre-illuminated to the extraordinary wave. The extraordinary pump will record a large variety of noisy gratings in the same manner as the ordinary wave does. The difference is that it is not possible to find among these noisy space-charge gratings those which are Bragg-matched to the two pump waves simultaneously (no gratings with grating vectors $\boldsymbol{K}_1$ and $\boldsymbol{K}_2$). This can be easily seen from Fig. 6b where apart from the wavevector of the extraordinary pump wave the wavevectors for several arbitrarily chosen scattered extraordinary waves are shown by dashed arrows. Not one of these scattered waves (and no other scattered extraordinary wave) can record gratings with grating vectors $\boldsymbol{K}_1$ and $\boldsymbol{K}_2$. This explains why the pre-exposure to the extraordinary wave can not improve the conditions for observation of the transient scattering (compare the peak values in Fig. 3a and 3b which are practically indistinguishable). Moreover, because of partial depletion of the extraordinary wave (a considerable part of its intensity is feeding the famous beam fanning [7] in $BaTiO_3$) the transient scattering can be even inhibited as compared to the case A with both pump waves switched on simultaneously.

The ultimate intensity of the transient peak depends also on the value of the integral in (6), which in turn depends on the absolute value of the coupling coefficient Γ (imaginary for the transient scattering). The theory [2–4] says that Γ is a function of the pump intensity ratio $r = \boldsymbol{I}_{\mathrm{p}}^{\mathrm{o}}/\boldsymbol{I}_{\mathrm{p}}^{\mathrm{e}}$. We fit (3) to the measured pump ratio dependence of the transient peak intensity and find $(\alpha_{\mathrm{o}}/\alpha_{\mathrm{e}}) = 0.85 \pm 0.05$ as a fitting parameter. This value agrees fairly well with the directly measured value of $(\alpha_{\mathrm{o}}/\alpha_{\mathrm{e}}) \approx 0.9 \pm 0.1$ for our $BaTiO_3$ sample .

3 Conclusions

From the time of publication of the first article of Magnussen and Gaylord on conical scattering in photorefractive crystals [8] it has been well known that the exposure of a photorefractive crystal to a coherent light wave results in recording of an infinite number of space-charge noisy gratings which can be partially visualized by the diffraction of the probe beam incident at different angles to the sample. It is shown in this paper that, being relatively weak (with small absolute values of the diffraction efficiency), these gratings can enhance by several orders of magnitude the intensity of radiation seeding the light-induced scattering, which results in a considerable enhancement of the non-linear scattering, too.

The enhancement of the amplified signal that is due to the larger seed radiation is not unusual by itself, it was already discussed for other parametric processes as, for example, subharmonic generation [9, 10]. A qualitatively new feature of the observed phenomenon is the strong sensitivity to the polarization of the pre-exposure beam. There are two pump waves in this type of scattering that are equally important from the point of view of ultimate gain for the seeding waves. To ensure the largest possible gain in the sample which is not dichroic the one-to-one pump intensity ratio should be chosen (see (3)). This symmetry is broken if we consider the contribution of differently polarized pump waves in the formation of the seeding radiation.

Acknowledgements. We are grateful to Prof. B. Sturman for stimulating discussions. One of us (S.O.) wishes to acknowledge the hospitality of the Laboratoire de Physique during his stay as a visiting professor at the Université de Bourgogne.

References

1. S. Odoulov, B. Sturman, L. Holtman, E. Kraetzig: Appl. Phys. B **52**, 317 (1991)
2. S. Odoulov, B. Sturman, L. Holtman, E. Kraetzig: J. Opt. Soc. Am. B **9**, 1648 (1992)
3. B. Sturman, S. Odoulov, U. van Olfen, E. Kraetzig: Appl. Phys. A **55**, 65 (1992)
4. B. Sturman, S. Odoulov: Sov. Phys. JETP **75**, 214 (1992)
5. M. Abramovitz, I.A. Stegun (Eds.): *Handbook of Mathematical Functions* (National Bureau of Standards, Washington, DC 1964)
6. S.H. Wemple, M. DiDomenico, Jr., I. Camlibel: J. Phys. Chem. Solids **29**, 1797 (1968)
7. J. Feinberg: J. Opt. Soc. Am. **72**, 46 (1982)
8. R. Magnussen, T. Gaylord: Appl. Opt. **13**, 1545 (1974)
9. D.C. Jones, L. Solymar: Opt. Lett. **14** 743 (1989)
10. S. Odoulov, R. Jungen, T. Tschudi: J. Opt. Soc. Am. B **11**, 1786(1994)